Active Geodesics: Region-based Active Contour Segmentation with a Global Edge-based Constraint

Vikram Appia   Anthony Yezzi
Georgia Institute of Technology,
Atlanta, GA, USA.

Abstract

We present an active geodesic *contour model in which we constrain the evolving active contour to be a geodesic with respect to a weighted edge-based energy through its entire evolution rather than just at its final state (as in the traditional* geodesic active contour *models). Since the contour is always a geodesic throughout the evolution, we automatically get local optimality with respect to an edge fitting criterion. This enables us to construct a purely region-based energy minimization model without having to devise arbitrary weights in the combination of our energy function to balance edge-based terms with the region-based terms. We show that this novel approach of combining edge information as the* geodesic constraint *in optimizing a purely region-based energy yields a new class of active contours which exhibit both local and global behaviors that are naturally responsive to intuitive types of user interaction. We also show the relationship of this new class of globally constrained active contours with traditional minimal path methods, which seek global minimizers of purely edge-based energies without incorporating region-based criteria. Finally, we present some numerical examples to illustrate the benefits of this approach over traditional active contour models.*

1. Introduction

Partial differential equations (PDE) based curve evolution models have been used extensively for image segmentation ever since they were introduced by Kass *et al.* in [9]. The model is sensitive to initialization because it uses a local gradient-based edge detector to stop the evolving curve on object boundaries. Level set based implicit curve evolution approaches were later developed [4, 10] to overcome the major drawbacks of the classical active contour model: *parameterization* and *topological changes*.

Cohen and Kimmel [8] converted the energy minimization problem into a cost accumulation problem, which can generate global minimal paths between two end points. Using these minimal paths Cohen and Kimmel present an interactive edge-based segmentation algorithm that can be initialized by a single point on the object boundary. Later, Appleton and Talbot [3] used minimal paths to develop an interactive segmentation algorithm which is initialized by a single user given point inside the object of interest. They modify the edge metric by making it inversely proportional to the distance from the point inside the object of interest and induce a cut in the image domain to find the globally optimal geodesic. For more details on the globally optimal geodesic active contour (GOGAC) model, we refer the reader to [3].

Region-based curve evolution techniques, which were developed later, define energy functionals based on region statistics rather than local image gradient. The Mumford and Shah model [11], which approximates the image to a piece-wise smooth representation forms the basis for various region statistics based segmentation algorithms [13,14]. Chan and Vese [6] developed a mean-curvature flow based level set implementation of a specific case of the Mumford-Shah energy functional, where the mean intensity of the pixels inside and outside the curve are used as a smooth approximation of the image.

Majority of the segmentation algorithms use either edge- or region-based energy minimization. Edge-based segmentation algorithms have better precision on the edges along the object boundary, whereas region-based segmentation algorithms are less susceptible to local minima. Paragios *et al.* [12] combine a probability based active region model to the classical edge-based model and Chakraborty *et al.* [5] developed a game-theory based approach to combine region and edge-based models in an attempt to exploit the benefits of both the approaches.

In this paper, we present a region-based active contour model with a global edge-based constraint. We constrain our geodesic to be a closed geodesic throughout the evolution, which enables us to devise a purely region-based energy minimization. We call this constrained closed geodesic *active geodesic*. The global edge-based constraint ensures local optimality on the weighted edge-based energy, rather than a compromise between a weighted edge- and region-based energy. Thus, the *active geodesic* exhibits local and global optimality not only in the final converged state, but throughout the curve evolution process.

We also develop an interactive segmentation algorithm based on this *active geodesic* contour model. The user initializes the algorithm by placing a pole to identify the object of interest. Subsequently the user can interact with the algorithm, if necessary, by placing additional poles and zeros to repel or attract the *active geodesic* towards the desired edges. These poles and zeros vary the weighted edge-based energy locally, which in turn has a global effect on the *active geodesic*.

2. Coupling Region- and Edge-based Segmentation

2.1. Edge-based Segmentation using Minimal Paths

The minimal path [8] approach is designed to extract the shortest path between two points on an image (grid) for a given traveling cost function. The Eikonal equation used to solve the minimal path problem can be defined as

$$\|\nabla u\| = \tau, \tag{1}$$

where $\tau(x)$ is the traveling cost at a given grid point and $u(x)$ is the accumulated cost. For edge-based minimal paths, we use an edge-based traveling cost function

$$\tau(x) = g\left(\frac{1}{1+\|\nabla I\|}\right) + \epsilon, \tag{2}$$

where $g(\cdot)$ is a monotonically increasing function, $\epsilon > 0$ is a regularizer and ∇I is the gradient of the image at a given location. To extract the shortest path between two points, we calculate u by propagating wavefronts from one of the two points (source point) to the other (end point). Then, by following the gradient descent in the vector field $\vec{\nabla u}$, we trace our path back to the source point. This path is the globally optimal open geodesic between the two points.

The minimal path approach uses Fast Marching Method (FMM) [1] to solve the Eikonal equation numerically on Cartesian grids. FMM is a computationally efficient single-pass algorithm designed to solve the Eikonal equation. Recently, authors in [2] proposed an Isotropic Fast Marching scheme, which is the most accurate numerical implementation of Eikonal equation to date. In all our experiments, we will use this Isotropic Fast Marching scheme.

2.1.1 Detecting Closed Curves using Minimal Paths

If two different global minimal paths exist between two points on the image, the two open geodesics will complete a closed contour. Now, consider a single source point given in the image domain. To detect closed curves, we have to find points on the domain from which two global minimal paths (back to the single source) exist, *i.e*, the two paths have the same accumulated cost. These special points are called saddles of u, and they can be interpreted as the points where the propagating fronts collide. To detect saddle points we use the technique described in [7].

In the cardiac image shown in Figure 1(a), we place the source point (marked 'X') on the object boundary. Figure 1(b) shows the level set representation of the wavefronts propagating from the source. Figure 1(c) and Figure 1(d) show the various detected saddle points and the closed curves associated with each detected saddle point.

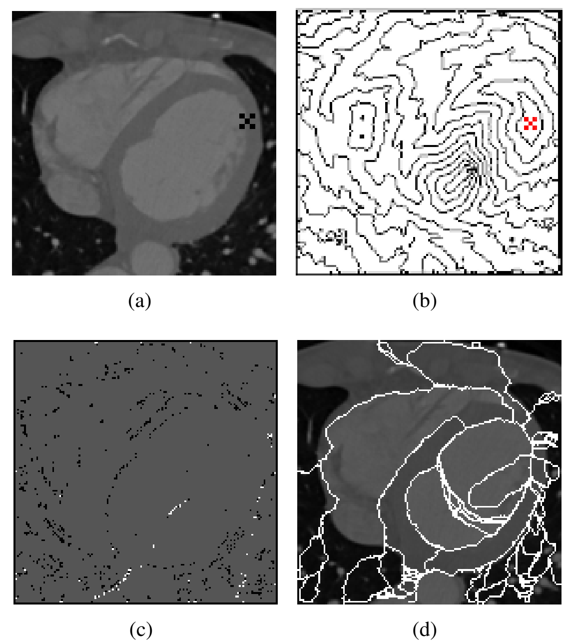

Figure 1. (a) Cardiac image with source point marked by an 'X'. (b) Level set representation of the propagating wavefronts. (c) The white pixels in the image indicate saddle points. (d) Closed curves associated with each saddle point.

2.2. Shock Curves

Figure 2(a) shows an illustration of the fronts emanating out of the source in different directions. Each gray level indicates a different neighbor of the source point from which the front at any given location propagated from. We observe that the fronts arriving from two different directions will form shock curves when they meet. By definition, the locations on these shock curves where the fronts arrive from two exactly opposite directions (collide) are the saddle points. The minimal paths from saddle points lying on the shock curves will arrive at the source from two different direc-

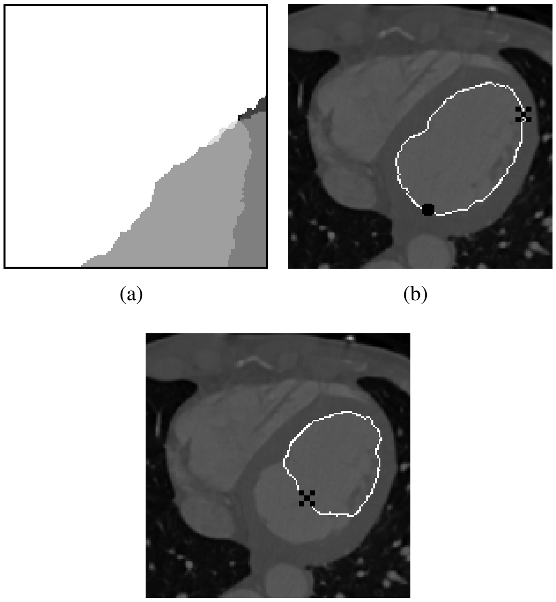

(a) (b) (c)

Figure 2. (a) Each gray level indicates a different neighbor of the source point from which the front at the given location propagated. The intersection of these labeled regions will form shock curves. (b) Closed curve with minimum region-based energy. The source point is marked by an 'X' and the saddle point by a 'dot'. (c) Segmentation with source point lying inside the object of interest.

tions, forming a closed geodesic. The minimal paths from all other points along the shock curve will also arrive at the source from two different directions, but the two paths will not have the same accumulated cost. Saddle points are isolated points on a shock curve which form curves that are closed geodesic at the shock curve.

2.3. Incorporating Region-based Energy

The next step is to choose the appropriate saddle point to segment the object. For this, we assume that the object surrounded by an edge also exhibits certain region-based (statistical) properties. We can now compare the region-based energy of all detected closed geodesics. Let us consider the Chan-Vese [6] energy function of the form

$$E = (I-\mu)^2 + (I-\nu)^2, \tag{3}$$

where μ is the mean of pixel intensities inside the curve and ν is the mean of pixel intensities outside the curve. Among all detected closed curves, the curve with the minimum region-based energy will segment the object. From the various geodesics shown in Figure 1(d), the closed geodesic with the minimum region-based energy segments the left ventricle as shown in Figure 2(b).

Until this point, we assumed that our source point was on the boundary of the object of interest. This meant that the saddle point associated with the closed geodesic exhibiting least region-based energy also fell on the object boundary. Consider the source point shown in Figure 2(c), which is placed away from the object boundary. The segmentation obtained using the approach described previously does not segment the object (left ventricle). Thus, for a given source point, the minimal path approach guarantees the global minimum for edge-based energy, but it does not guarantee that the closed curve will also correspond to the minimum of the region-based energy.

3. Global Edge-based Constraints for Region-based Active Contours

We use the region-based energy of the closed geodesic to perturb the saddle point along the shock curve, which indirectly evolves the closed geodesic. Thus, the curve evolution has only two degrees of freedom, the two co-ordinates of the saddle point. We continue evolution until we reach a minimum for the region-based energy. The minimal path approach ensures that our segmentation evolves based on region-based energy with an in-built edge-based optimality.

Let S denote the saddle point on the given curve C. The shock curve corresponding to S will form a boundary of the vector field $\vec{\nabla} u$ in the image plane. We parametrize the boundary (shock curve) with a linear function $\psi(x) = p$. By solving

$$\nabla\psi \cdot \nabla u = 0, \tag{4}$$

we propagate ψ in the direction of the characteristics of $\vec{\nabla} u$ to form a level set function in the image domain. This level set function ψ forms an implicit representation of the curve C. If we choose a function such that $\psi(S) = 0$, then the closed geodesic will be embedded as the zero level set of ψ.

Now, consider a general class of region-based energies,

$$E(C) = \int_\Omega f(x)dA. \tag{5}$$

We can represent the gradient of $E(C)$ w.r.t the parameter p as the line integral

$$\nabla_p E = \int_C f \cdot \nabla_p C \cdot \vec{N} ds, \tag{6}$$

where s is the arc length parameter of the curve and $\vec{N}$ is the outward normal to the curve C. Since ψ is a function of the parameter p as well as the curve C, we have

$$\psi(C, p) = p. \tag{7}$$

Taking the gradient of (7), we get

$$\nabla\psi \cdot \nabla_p C = 1 \Rightarrow \frac{\nabla\psi}{\|\nabla\psi\|} \cdot \nabla_p C = \frac{1}{\|\nabla\psi\|}$$
$$\Rightarrow \nabla_p C \cdot \vec{N} = \frac{1}{\|\nabla\psi\|}. \tag{8}$$

Since C is embedded in the level set function ψ, both C and ψ have the same outward normal, $\vec{N} = \frac{\nabla\psi}{\|\nabla\psi\|}$. Thus, substituting (8) in (6) we get

$$\nabla_p E = \int\limits_C \frac{f}{\|\nabla\psi\|} ds. \tag{9}$$

The factor of $\|\nabla\psi\|$ in the denominator of the line integral varies the contribution of each point on the curve. The points on C closer to the saddle point will have a higher contribution to the integral than the points further away.

For the Chan-Vese [6] energy model described in (3), f takes the form

$$f = 2(\mu - \nu)\{I - \frac{\mu + \nu}{2}\}. \tag{10}$$

We now perturb the saddle point S along the shock curve, against the gradient $\nabla_p E$. The value of the line integral in (9) governs how far along the shock curve we perturb the saddle point. Once we perturb the saddle point, the two open geodesics back to the source from the new location cease to form a closed geodesic. Thus, we make the perturbed saddle point (at the new location) our new source. We now recompute u from this new source point and pick a saddle point satisfying the following two conditions:

1. The associated closed geodesic has lower region-based energy when compared to the energy of the closed geodesic obtained prior to perturbing the saddle point.

2. It lies closest to the previous source point.

The accumulated cost (u) from the previous iteration is used as the metric to measure the distance from the previous source point and not the Euclidean distance. Since we move the saddle point against the gradient of E, the region-based energy for the closed geodesic will decrease with each evolution of the curve. We follow this procedure until we converge to a minimum for the region-based energy.

4. Interactive Segmentation Algorithm

Using the *active geodesic* contour evolution, we present an interactive segmentation algorithm. By placing poles and zeros the user can attract/repel the *active geodesic* towards a desired segmentation.

4.1. Attractors and Repellers

We refer to the poles and zeros placed by the user as *repellers* and *attractors*, respectively. For each repeller (P) and attractor (Z) the user places, we update the traveling cost function as

$$\tau'(x) = \tau(x) \circ h_1\Big(\frac{1}{distance(x, P)}\Big), \tag{11}$$

$$\tau'(x) = \tau(x) \circ h_2\Big(distance(x, Z)\Big), \tag{12}$$

where h_1 and h_2 are monotonically increasing functions, the '$\circ$' operator represents Hadamard product[1] and *distance*$(\cdot, \cdot)$ is the Euclidean distance. By placing these *attractors* and *repellers* the user is locally modifying the traveling cost (weighted edge function). This local variation has a global effect on the *active geodesic* evolution as we see in the examples in Section 5.

4.2. Algorithm details

We initialize the algorithm by asking the user to place a *repeller* inside the object of interest. This artificially placed pole serves the following two purposes:

1. It identifies the object of interest.

2. It ensures that the propagating wavefronts wrap around the pole to generate a family of closed geodesics.

Now, we randomly pick a point in the vicinity of the *repeller* (different from the pole) as the source point, and follow the procedure described in Section 3. In the very first iteration we do not have a reference for the source from previous iteration, hence we choose the saddle point closest to the *repeller*. We move the saddle point against the gradient $\nabla_p E$ to minimize the region-based energy of the closed geodesic. This saddle point becomes the source for the second iteration. We continue the evolution until we converge to a minimum. Figure 3 shows the evolving closed geodesic and the final segmentation of the left ventricle.

Once we converge to a minimum, we present the user with the resultant closed geodesic. If the user is not satisfied, he can add an *attractor* or a *repeller* to drive the geodesic towards the desired edges. Consider the segmentation result shown in Figure 4(a). Placing another *repeller* inside the closed geodesic further evolves the closed geodesic away from the new *repeller* as shown in Figure 4(b).

The *repellers* placed by the user are classified as interior or exterior *repellers* based on their location with respect to the current state of the *active geodesic*. We choose only those saddle points, which form closed geodesics that separate all the interior *repellers* from the exterior *repellers*. Thus, a *repeller* placed inside the closed curve stays inside the final segmentation and a *repeller* placed outside the closed curve stays outside the final segmentation. Figure 6(b) shows the final desired right ventricle segmentation.

5. Experimental Results

In this section, we compare the segmentation results of our region-based *active geodesic* model to the purely region-based Chan-Vese segmentation model and the purely

[1] Hadamard product is the entry-wise product of two matrices. For two given matrices A_{mxn} and B_{mxn}, $(A \circ B)_{i,j} = (A)_{i,j} \cdot (B)_{i,j}$.

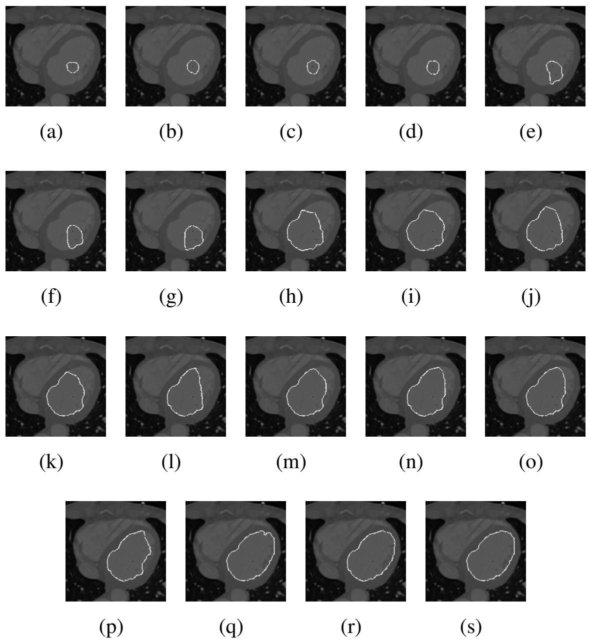

Figure 3. (a) Segmentation after the first iteration. (b-r) Evolution of the closed curve to minimize the region-based energy. (s) Final converged segmentation after 19 iterations.

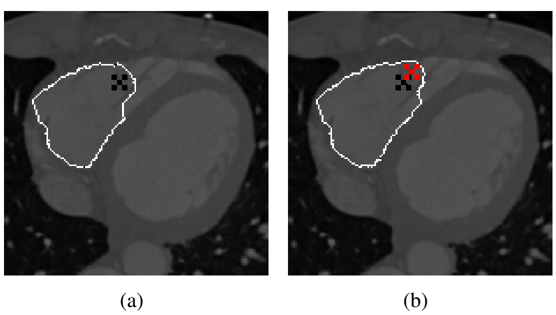

Figure 4. Initial *repeller* is marked by a black 'X'. (a) Converged segmentation of the right ventricle with the initial *repeller*.(b) Converged segmentation with the second *repeller* (Red 'X').

edge-based segmentation approach described in [3]. For the Chan-Vese model, we use level set based curve evolution to minimize the energy in Equation (3). For the GOGAC model [3], we modify our edge-based traveling cost to

$$\tau'(x) = \frac{1}{r}\left(g\left(\frac{1}{1+\|\nabla I\|}\right)+\epsilon\right), \tag{13}$$

where r is the Euclidean distance from the user specified-point. By inducing a cut in the image domain, we obtain the globally optimal segmentation. In Figure 5, we compare the segmentation of the right ventricle with the same initialization, but four different orientations of the cut. We see that the final segmentation depends on the orientation of the cut.

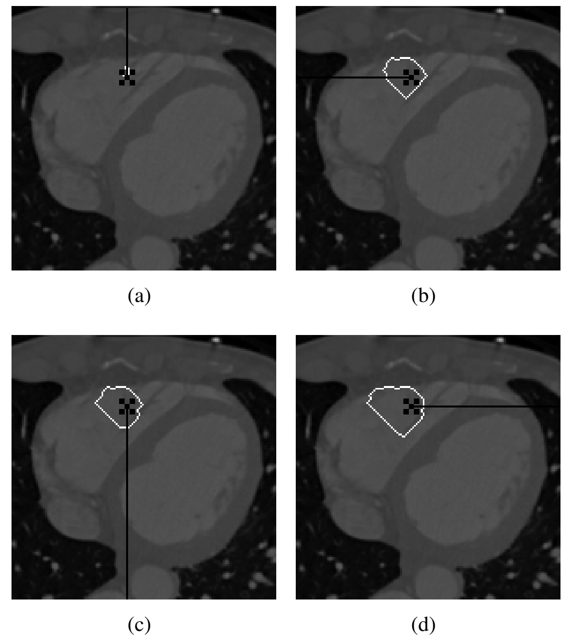

Figure 5. The segmentation of the right ventricle using GOGAC varies with the orientation of the cut.

In Figure 6, we compare segmentation of the two ventricles in a cardiac image. We are able to segment the right ventricle after modifying the metric by placing a few *attractors* and *repellers* (Figure 6(b). The region-based Chan-Vese model does not depend on edges. Thus, it fails to segment both the ventricles as shown in Figure 6(d).

In Figure 7, we compare the segmentation of a cell with multiple nuclei. Using our approach the user can segment the cell by placing additional *attractors* and *repellers* (Figure 7(a)). The final segmentation using GOGAC approach and the purely region-based Chan-Vese model are shown in Figures 7(b) and 7(c), respectively.

6. Conclusion

We have presented a novel *active geodesic* contour model, which constrains the evolving active contour to be a geodesic with respect to a weighted edge-based energy throughout the evolution process. Minimizing region-based energy with this constraint yields closed geodesics that exhibit both local and global behaviors. *Active geodesics* are also naturally responsive to intuitive user interactions and we use them to develop an interactive segmentation algorithm. We conclude with results illustrating the benefits of our approach over the traditional active contour models.

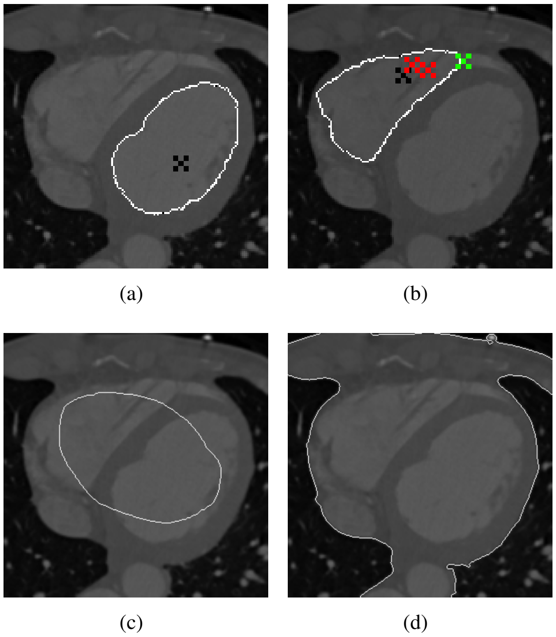

Figure 6. Initial *repeller* is marked by a black 'X'.(a) Left Ventricle segmentation after 19 iterations. (b) Right Ventricle segmentation after the user has placed a few *attractors* (marked by green 'X's) and *repellers* (marked by red 'X's). Desired segmentation in 27 iterations. (c) Initialization for the Chan-Vese segmentation. (d) Final region-based Chan-Vese segmentation.

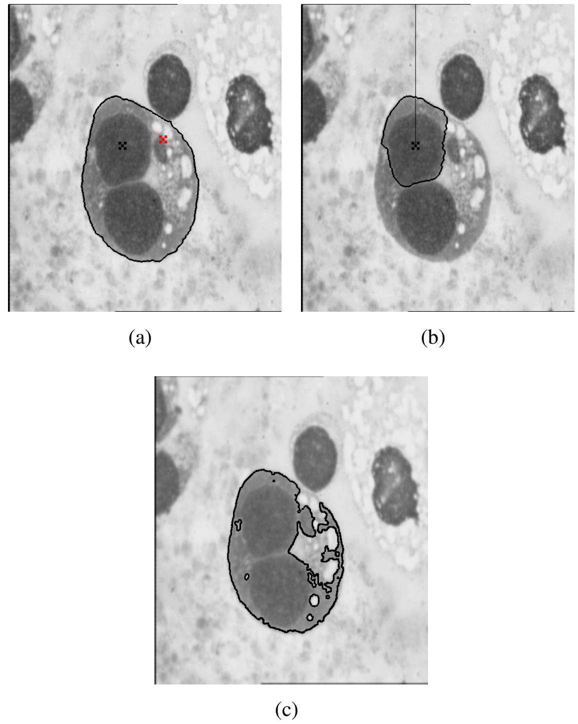

Figure 7. (a) Initial *repeller* is marked by a black 'X'. Subsequent *attractors* are marked by green 'X's and *repellers* are marked by red 'X's. Desired segmentation in 22 iterations. (b) Cell segmentation results using edge-based GOGAC approach. (c) Final region-based Chan-Vese segmentation.

7. Acknowledgements

This work was supported by NIH (grant #R01-HL-085417) and NSF (grant #CCF-0728911).

References

[1] D. Adalsteinsson and J. A. Sethian. A fast level set method for propagating interfaces. *Journal of Computational Physics*, 118:269–277, 1994.

[2] V. Appia and A. Yezzi. Fully isotropic fast marching methods on cartesian grids. ECCV'10, pages 71–83, 2010.

[3] B. Appleton and H. Talbot. Globally optimal geodesic active contours. *J. Math. Imaging Vis.*, 23:67–86, July 2005.

[4] V. Caselles, R. Kimmel, and G. Sapiro. Geodesic active contours. *IJCV*, 22:61–79, February 1997.

[5] A. Chakraborty and J. S. Duncan. Game-theoretic integration for image segmentation. *IEEE Trans. Pattern Anal. Mach. Intell.*, 21(1):12–30, 1999.

[6] T. E. Chan and L. A. Vese. A level set algorithm for minimizing the mumford-shah functional in image processing. In *IEEE Workshop on Variational and Level Set Methods in Computer Vision*, pages 161–168.

[7] L. Cohen and R. Kimmel. Edge integration using minimal geodesics. Technical report, 1995.

[8] L. Cohen and R. Kimmel. Global minimum for active contour models: A minimal path approach. *International Journal of Computer Vision*, 24:57–78, 1997.

[9] M. Kass, A. Witkin, and D. Terzopoulos. Snakes: Active contour models. *IJCV*, 1(4):321–331, 1988.

[10] R. Malladi, J. A. Sethian, and B. C. Vemuri. Evolutionary fronts for topology-independent shape modeling and recovery. ECCV '94, pages 3–13, Secaucus, NJ, USA, 1994. Springer-Verlag New York, Inc.

[11] D. Mumford and J. Shah. Optimal approximations by piecewise smooth functions and associated variational problems. *Communications on Pure and Applied Mathematics*, 42(5):577–685, 1989.

[12] N. Paragios and R. Deriche. Coupled geodesic active regions for image segmentation: A level set approach. In *ECCV (2)*, pages 224–240, 2000.

[13] A. Tsai, Jr, and A. S. Willsky. Curve Evolution Implementation of the Mumford Shah Functional for Image Segmentation, Denoising, Interpolation, and Magnification. *IEEE Trans. on Image Processing*, 10(8):1169–1186, 2001.

[14] S. C. Zhu and A. Yuille. Region competition: Unifying snakes, region growing, and bayes/mdl for multi-band image segmentation. *IEEE Transactions on Pattern Analysis and Machine Intelligence*, 18:884–900, 1996.